

## Two-Body Photodisintegration of ${}^3\text{He}$ between 150 and 350 MeV

W. J. Briscoe, D. H. Fitzgerald, and B. M. K. Nefkens  
*University of California, Los Angeles, California 90024*

and

Hall Crannell and D. I. Sober  
*The Catholic University of America, Washington, D.C. 20064*

and

R. Goloskie  
*Worcester Polytechnic Institute, Worcester, Massachusetts 01609*

and

W. W. Sapp, Jr.  
*The Massachusetts Institute of Technology, Cambridge, Massachusetts 02139*  
 (Received 3 May 1982)

Differential cross sections for  ${}^3\text{He}(\gamma, d)p$  have been measured at  $\theta_p(\text{c.m.}) \sim 60^\circ$  and  $\sim 90^\circ$  for photon energies between 150 and 350 MeV. The data have an absolute normalization uncertainty of 6% and provide absolute differential cross sections suitable for a test of time-reversal invariance when used in conjunction with comparable data on the inverse reaction.

PACS numbers: 25.20.+y, 11.30.Er, 25.10.+s

Time-reversal invariance is a sufficient condition to relate any two-body reaction of unpolarized particles with its inverse reaction via detailed balance. Not all interactions are suitable to test time-reversal invariance, though. For example, detailed balance is assured by current conservation in electromagnetic interaction involving a nucleon on the mass shell.<sup>1</sup> No such restriction exists if the nucleon is excited to a resonance.<sup>1</sup> There is some evidence<sup>2</sup> that the  $\Delta(1232)$  intermediate state plays an important role in  ${}^3\text{He}(\gamma, d)p$  for  $200 \leq E_\gamma \leq 300$  MeV; thus, in this energy region one can test time-reversal invariance in  $\gamma^3\text{He} \rightarrow pd$ .

The published measurements of the two-body photodisintegration of  ${}^3\text{He}$ <sup>3-6</sup> at  $E_\gamma$  between 180 and 500 MeV differ by up to a factor of 3. The disagreement among the radiative capture measurements<sup>7-9</sup> in the same energy region is not as dramatic, but it is significant. The purpose of the experiment reported here is to provide an improved measurement of the cross section of  ${}^3\text{He}(\gamma, d)p$ . This measurement is part of a complete test of time-reversal invariance including measurements of  $p(d, \gamma){}^3\text{He}$  and  $d(p, \gamma){}^3\text{He}$  by an associated collaboration.<sup>10</sup>

In the present experiment absolute differential cross sections were obtained for  ${}^3\text{He}(\gamma, d)p$  at  $\theta_p(\text{c.m.}) \sim 60^\circ$  and  $\sim 90^\circ$ , and  $150 \leq E_\gamma \leq 350$  MeV. We emphasized techniques not employed in previ-

ous measurements. The use of a single-arm magnetic spectrometer avoids the acceptance matching required in coincidence experiments and allowed us to perform adjuvant electron scattering measurements under similar experimental conditions. The photon beams used in our measurements were not collimated and all photons produced in the radiator struck the target, ensuring no net polarization of the photons and simplifying the beam intensity calculations. The use of a gas target reduces the density corrections which are important for liquid- ${}^3\text{He}$  targets.

The measurement was performed at the Massachusetts Institute of Technology Bates Linear Accelerator<sup>11</sup> using the 900-MeV/c high-resolution spectrometer.<sup>12</sup>  ${}^3\text{He}(\gamma, d)p$  events were uniquely defined by measurement of the energy loss, range, scattering angle, and momentum of the deuteron. The focal-plane detector system<sup>13</sup> consisted of three multiwire drift chambers<sup>14</sup> and a stack of five plastic scintillators. For each event the raw chamber information and the pulse heights and relative timing of the scintillator signals were recorded. Proton, deuteron, and triton events are clearly separated in pulse height in each counter, and a background-free sample of deuterons is achieved when two or more counters are used in combination. The momentum of the deuteron was determined to  $\pm 0.2\%$ .

The target cell,<sup>15</sup> a vertical cylinder with a

uniform 0.4-mm aluminum wall, was cooled by contact with a liquid-nitrogen reservoir and operated at a pressure of  $\sim 1$  MPa ( $\sim 10$  atm). After filling, the cell was isolated from the filling system. The temperature of the gas was determined from the ratio of equilibrium pressures before and after cooling. The average equilibrium gas temperature and density were  $80 \pm 2$  K and  $0.465 \pm 0.015$  mg/cm<sup>3</sup>, respectively.

The effective target length and solid angle were defined by fixed tungsten slits near the target and a set of variable slits at the entrance to the spectrometer. The effective product of target length and solid angle was checked at each spectrometer setting by elastic scattering on <sup>3</sup>He. The measured cross sections agree to  $\pm 3\%$  with those obtained by Dunn.<sup>15</sup> Electron scattering also provided an independent check on the purity of the target. The <sup>4</sup>He contamination of the <sup>3</sup>He was thus determined to be  $\sim 0.8\%$ .

The bremsstrahlung beam was produced in a Ta radiator 235.4 mg/cm<sup>2</sup> [0.0354 radiation length (r.l.)] thick, situated 10 cm from the center of the target. While this arrangement precluded sweeping the electrons from the photon beam, it ensured that the entire bremsstrahlung beam hit the target. This simplified the calculation of the bremsstrahlung spectrum<sup>16</sup> and absolute intensity of the photon beam. The intensity of the electron beam was measured to within

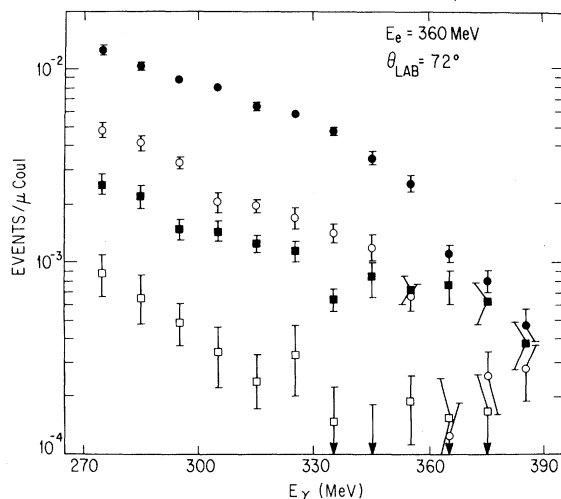


FIG. 1. The relative contributions of yields  $N_a$ , solid dots;  $N_b$ , open dots;  $N_c$ , solid squares; and  $N_d$ , open squares, as a function of  $E_\gamma$ . Above the photon end point each of these yields drops to approximately the same value, showing that the signal is background in that region.

$\pm 0.5\%$  by two toroid monitors located several meters upstream of the target.

Measurements were made at electron energies of 275, 300, 325, and 360 MeV at  $\theta_a(\text{lab}) = 72^\circ$  [ $\theta_p(\text{c.m.}) \approx 90^\circ$ ], and 210, 260, 310, and 360 MeV at  $\theta_a(\text{lab}) = 103^\circ$  [ $\theta_p(\text{c.m.}) \approx 60^\circ$ ]. The momentum acceptance of the spectrometer detection system was 6.4%. At each electron energy the spectrometer field was varied in 4% steps to span the deuteron momentum range corresponding to photon energies from  $\sim 5\%$  above the bremsstrahlung end point to approximately 100 MeV below the end point. Thus, overlapping measurements of the yield at different end-point energies were obtained for much of the data.

The presence of electrons in the photon beam

TABLE I. The tests listed provide experimental verification of the values of parameters and assumptions used in calculating the absolute differential cross section for <sup>3</sup>He( $\gamma, d$ )p. Tests 1–5 confirm the linear dependence of (i) spectrometer acceptance on entrance slit opening (1 and 2), (ii) target gas density on pressure (3), and (iii) relative bremsstrahlung flux on radiator thickness (4 and 5). Tests 4 and 5 also show the resulting cross section to be independent of radiator-related background. Test 6 confirms the absence of radiator-related rescattering backgrounds. Tests 7–10 provide a check on the absolute values used for effective target thickness, spectrometer solid angle, and the temperature and pressure of the target gas.

Test	Expected ratio	Measured ratio
(1) Halve vertical acceptance	0.50	$0.46 \pm 0.04$
(2) Halve horizontal acceptance	0.50	$0.49 \pm 0.04$
(3) Reduce gas pressure	0.54	$0.57 \pm 0.04$
(4) 0.066 59/0.035 38-r.l.-thick Ta radiator	1.76	$1.76 \pm 0.10$
(5) 0.013 65/0.035 38-r.l.-thick Ta radiator	0.40	$0.42 \pm 0.04$
(6) $d\sigma/d\Omega$ <sup>3</sup> He( $\gamma, d$ )p Cu and Ta radiator	1.00	$1.03 \pm 0.05$
(7) <sup>3</sup> He( $e, e$ ) $\theta_{\text{lab}} = 72^\circ$	1.00 <sup>a</sup>	$1.02 \pm 0.02$
(8) <sup>3</sup> He( $e, e$ ) $\theta_{\text{lab}} = 103^\circ$	1.00 <sup>a</sup>	$0.98 \pm 0.04$
(9) <sup>2</sup> H( $\gamma, p$ )n $\theta_{\text{lab}} = 72^\circ$	1.00 <sup>b</sup>	0.90 $0.90 \pm 0.08$ 1.06
(10) <sup>4</sup> He( $\gamma, t$ )p $\theta_{\text{lab}} = 103^\circ$	1.00 <sup>c</sup>	1.00 $0.98 \pm 0.03$

<sup>a</sup>Ref. 15.

<sup>b</sup>Refs. 17, 18, and 19.

<sup>c</sup>Refs. 4 and 20.

introduces contributions to the deuteron signal due to electrodisintegration of  $^3\text{He}$  and to photons produced in the target. In addition there are small sources of background due to photodisintegration in the target window and radiator. Four measurements are necessary at each spectrometer setting to extract the  $^3\text{He}(\gamma, d)p$  yield: (a) radiator in beam, target full ( $N_a$ ); (b) radiator out of beam, target full ( $N_b$ ); (c) radiator in beam, target empty ( $N_c$ ); (d) radiator out of beam, target empty ( $N_d$ ). The net  $^3\text{He}(\gamma, d)p$  yield is  $S_\gamma = N_a - N_b - N_c + N_d$ . The typical contributions of  $N_{a-d}$  are shown in Fig. 1. The degradation of electron energy in the radiator has  $\leq 1\%$  effect on  $S_\gamma$ . After subtraction of the measured background the residual signal above the end point is less than 1.5% (5%) of the average true signal below the end point at  $72^\circ$  ( $103^\circ$ ). There is excellent agreement among the cross sections evaluated at different bremsstrahlung end-point energies.

Some photodisintegration yields were also measured for  $^2\text{H}$  and  $^4\text{He}$ . These measurements provided a further check on the bremsstrahlung spectrum calculation and the normalization factors. The result of the  $d(\gamma, p)n$  measurement is in agreement with previous measurements,<sup>17-19</sup>

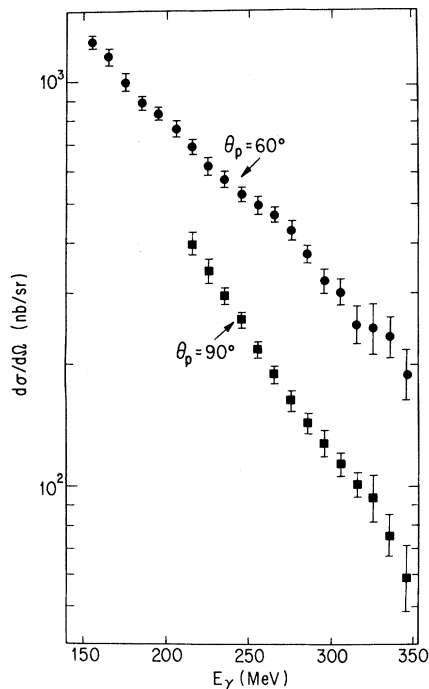


FIG. 2. The differential cross sections obtained in this experiment interpolated to  $\theta_p(\text{c.m.}) = 60^\circ$  and  $90^\circ$ . The errors shown are statistical only.

though the spread in the published data limits the sensitivity of this test to  $\pm 8\%$ . The cross sections obtained for  $^4\text{He}(\gamma, t)p$  agree with those of Argan *et al.*<sup>4</sup> and Arends *et al.*<sup>20</sup> The background due to the 0.8%  $^4\text{He}$  impurity in the  $^3\text{He}$  gas was evaluated from measurements of the  $^4\text{He}(\gamma, d)$  yield.

Several tests were performed to check the background subtraction procedure and the normalization factors. Radiator thickness, spectrometer apertures, target density, and  $Z$  of the radiator were varied with no effect on the cross section to  $\pm 8\%$ . The results of these tests are summarized in Table I.

The measured differential cross sections are shown in Fig. 2. The data within 10 MeV of each end point have been omitted because of the uncertainty in the calculated bremsstrahlung spec-

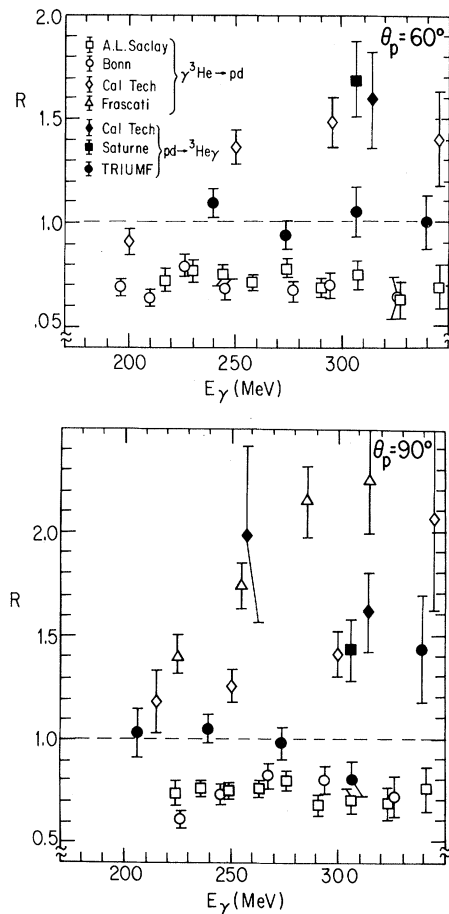


FIG. 3. The ratios ( $R$ ) of the  $d\sigma/d\Omega$ 's obtained in measurements of  $^3\text{He}(\gamma, p)d$ , open symbols (Refs. 4, 3, 6, 5, respectively), and  $d(p, \gamma)^3\text{He}$ , solid symbols (Refs. 9, 7, 8, respectively), to our results.

trum. Corrections to the data have been made for (i) local changes in the gas density due to beam heating (4.4%), (ii) signal due to  $^4\text{He}$  contamination (2.6%), (iii) loss of deuterons in the detection system (1.5%), and (iv) total dead time (1%–8%). The errors indicated are statistical only and do not include a 6% systematic uncertainty. The largest contributions to the systematic uncertainty are the uncertainties in the product of solid angle and target areal density ( $\pm 4\%$ ), and the calculation of the bremsstrahlung spectrum ( $\pm 2\%$ ).

The present results are compared with earlier results for  $^3\text{He}(\gamma, p)d$  and  $d(p, \gamma)^3\text{He}$  in Fig. 3. For this comparison our data were corrected ( $< 6\%$ ) for small changes in the c.m. angle with incident photon energy. The average ratios of previously published cross sections to ours are 0.69,<sup>3</sup> 0.73,<sup>4</sup> and 1.16,<sup>6</sup> at  $\theta_p(\text{c.m.}) = 60^\circ$ , and 0.71,<sup>3</sup> 0.74,<sup>4</sup> 1.67,<sup>5</sup> and 1.30,<sup>6</sup> at  $\theta_p(\text{c.m.}) = 90^\circ$ .

The 6% systematic uncertainty in our data represents a considerable improvement over those of previous measurements. While the disagreements among the present results and those of Refs. 3 and 4 are outside statistical uncertainties, the relatively large systematic uncertainties of these experiments, 10%–15%,<sup>3</sup> and 10%,<sup>4</sup> mitigate the severity of these disagreements. However, the results of Refs. 5 and 6 cannot be reconciled with our data.

As can be seen in Fig. 3 our data strongly disagree with the measurements of the inverse reaction of Refs. 7 and 9; however, they agree at seven out of nine points with the preliminary data of Ref. 8. In view of the well-established absolute normalization in the present measurement, a large disagreement between these data and measurements of the inverse reaction has serious implications. Two new measurements<sup>8,10</sup> of  $d(p, \gamma)^3\text{He}$  have been completed. Therefore, it is appropriate to defer evaluation of our results in terms of a test of time-reversal invariance until these data<sup>8,10</sup> are published in final form.

We acknowledge the efforts and support of the linac staff and ( $\gamma, p$ ) group at Massachusetts Institute of Technology Bates Linear Accelerator. We thank N. Kalantar-Nayestanaki, R. S. Turley,

B. C. Craft, III, and R. Schumacher for their assistance, and A. W. Stetz for supplying information on the preliminary results of Ref. 8. One of us (D.I.S.) acknowledges the hospitality of the Technische Hochschule Darmstadt during part of this work. This work was supported in part by the U. S. Department of Energy and the National Science Foundation.

<sup>1</sup>J. Berstein, G. Feinberg, and T. D. Lee, Phys. Rev. 139, B1650 (1965).

<sup>2</sup>B. M. K. Nefkens *et al.*, Nucl. Phys. A353, 99c (1981), and summarized by P. L. Walden, Nucl. Phys. A374, 277c (1982).

<sup>3</sup>H. J. Gassen *et al.*, Z. Phys. A 303, 35 (1981).

<sup>4</sup>P. E. Argan *et al.*, Nucl. Phys. A237, 447 (1975).

<sup>5</sup>P. Picozza *et al.*, Nucl. Phys. A157, 190 (1970).

<sup>6</sup>C. A. Heusch *et al.*, Phys. Rev. Lett. 37, 405 (1976); K. T. McDonald, Ph.D. thesis, California Institute of Technology, 1972 (unpublished).

<sup>7</sup>B. M. K. Nefkens *et al.*, Phys. Rev. Lett. 45, 168 (1980).

<sup>8</sup>J. M. Cameron *et al.*, in Abstracts of the Proceedings of the Ninth International Conference on High Energy Physics and Nuclear Structure, Versailles, France, 1981 (unpublished), p. 473; A. W. Stetz, private communication.

<sup>9</sup>C. A. Heusch *et al.*, Phys. Rev. Lett. 37, 409 (1976); R. V. Kline, Ph.D. thesis, California Institute of Technology, 1973 (unpublished).

<sup>10</sup>B. M. K. Nefkens *et al.*, to be published.

<sup>11</sup>C. P. Sargent, W. Turchinets, and J. N. Weaver, IEEE Trans. Nucl. Sci. 22, 1341 (1975).

<sup>12</sup>W. Bertozzi *et al.*, Nucl. Instrum. Methods 162, 211 (1979).

<sup>13</sup>E. R. Kinney *et al.*, Nucl. Instrum. Methods 185, 189 (1981).

<sup>14</sup>W. Bertozzi *et al.*, Nucl. Instrum. Methods 141, 457 (1977).

<sup>15</sup>P. C. Dunn, Ph.D. thesis, Harvard University, 1980 (unpublished).

<sup>16</sup>J. L. Matthews and R. O. Owens, Nucl. Instrum. Methods 111, 57 (1973).

<sup>17</sup>D. I. Sober *et al.*, Phys. Rev. Lett. 22, 430 (1969).

<sup>18</sup>P. Dougan *et al.*, Z. Phys. A 276, 55 (1976), and 280, 341 (1977).

<sup>19</sup>R. L. Anderson, R. Prepost, and B. H. Wiik, Phys. Rev. Lett. 22, 13 (1969).

<sup>20</sup>J. Arends *et al.*, Nucl. Phys. A322, 253 (1979).